Environmental Guardian
https://www.sciltp.com/journals/eg

Article

Effective Removal of Malachite Green Dye on Camellia Sinensis Ash

Santosh Kumar [1,†], Nidhi Rai [1,2,†], Sanju Soni [1], Sonu Kumar [1], Aazad Verma [1] and Charu Arora [1,*]

[1] Department of Chemistry, Guru Ghasidas Vishwavidyalaya, Bilaspur 495009, India
[2] Department of Chemistry, IILM University, Greater Noida 201306, India
* Correspondence: charuarora77@gmail.com
† These authors contributed equally to this work.

How To Cite: Kumar, S.; Rai, N.; Soni, S.; et al. Effective Removal of Malachite Green Dye on Camellia Sinensis Ash. *Environmental Guardian* **2026**, *1*(1), 3.

Received: 4 July 2026
Revised: 9 August 2026
Accepted: 25 August 2026
Published: 7 September 2026

Abstract: This study investigates the efficacy of *Camellia sinensis* ash (tea powder/waste ash) as an adsorbent for removing Malachite Green (MG) dye from aqueous solutions. Comprehensive analyses, including SEM, XRD, BET surface area, and FTIR, were conducted to characterise the adsorbent. Key parameters influencing adsorption, such as pH, temperature, initial dye concentration, contact time, and adsorbent dosage, were systematically evaluated. Results indicated that at 30 °C, tea ash removed approximately 95.87% of MG dye from a 25 mg/L solution, with optimal performance observed in alkaline conditions. Column experiments revealed a maximum adsorption capacity of 75.02 mg/g. The Temkin isotherm model best described the adsorption equilibrium with a high correlation coefficient of 0.95. Thermodynamic analysis indicated an endothermic, spontaneous process; kinetic data best fit the pseudo-first-order model, consistent with physisorption.

Keywords: malachite green; tea ash; Temkin isotherm; adsorptive removal; pseudo-first-order kinetics model; physisorption

1. Introduction

Access to clean and safe drinking water has become an increasingly pressing issue worldwide. One of the most significant challenges we face in this regard is water pollution, which has severe and far-reaching consequences. As freshwater is a crucial resource for humans and wildlife alike, its degradation poses a severe risk to ecosystems and public health. The discharge of dye-contaminated wastewater poses significant environmental and public health risks, including the destruction of aquatic ecosystems, contamination of groundwater, and adverse impacts on human health [1–4]. The presence of synthetic dyes in wastewater is a challenging issue that requires efficient and effective treatment methods (Figure 1). Malachite green (MG) dye is a synthetic dye used in various industrial processes and as a coloring agent in the textile, paper, leather, and plastics industries [5–8]. The use of malachite green dye has been linked to several adverse effects that pose significant health hazards to humans, animals, and the environment. One of the most significant concerns regarding malachite green dye is its toxicity and potential carcinogenicity. Exposure to malachite green dye is known to cause genetic mutations, DNA damage, and an increased risk of cancer in humans and animals. This dye is known to be harmful to the liver and kidneys, leading to liver and kidney damage or failure. Malachite green dye is toxic to aquatic organisms such as fish, invertebrates, and plants. The dye can cause a decrease in their reproductive capacity, growth, and survival, leading to ecosystem imbalances and the loss of biodiversity. Continued exposure to malachite green dye can also lead to the accumulation of this dye in the environment, persistent organic pollutants, and the transfer of these pollutants to humans and animals through the food chain [9–11].

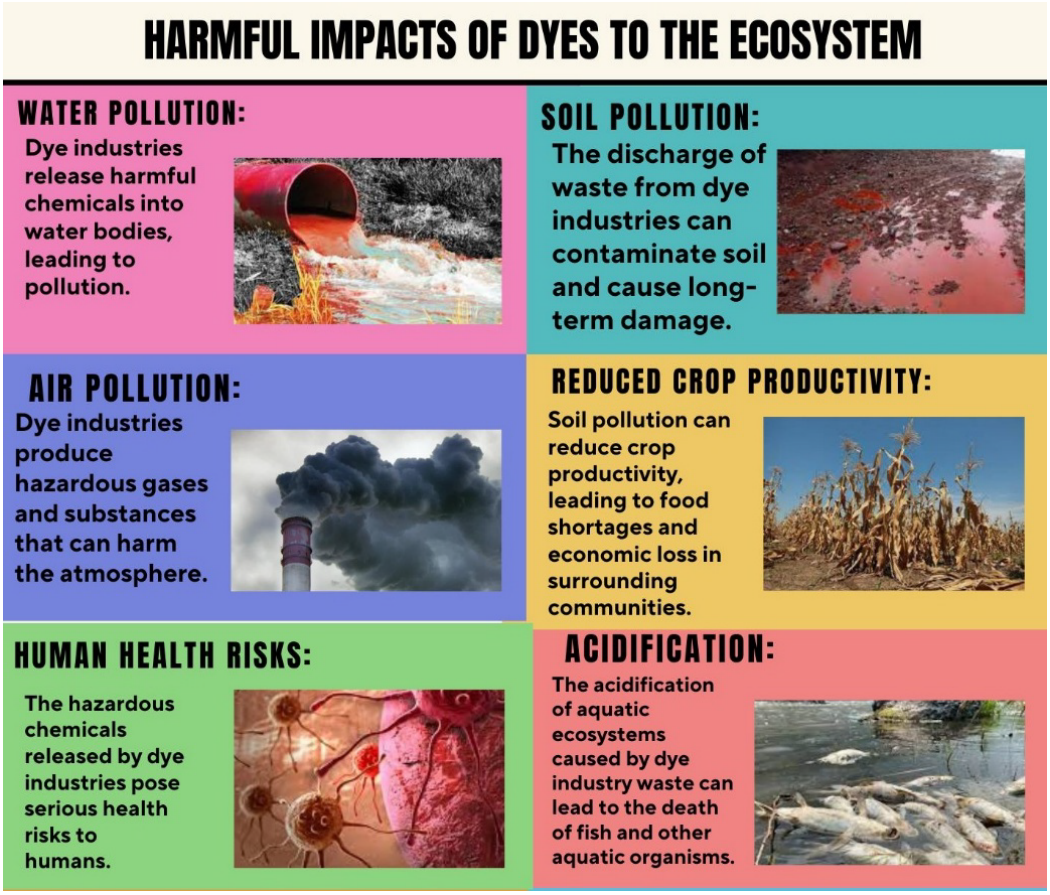

Figure 1. Dye pollution and its toxic effect.

Various treatment methods have been employed, including chemical precipitation, adsorption, membrane filtration, and biological treatment [12–16]. The choice of the optimal treatment method depends on several factors, including the type of dye, the wastewater composition, and the desired effluent quality. It is critical to adopt sustainable practices in industries that use dyes to minimize the release of dye-contaminated wastewater into the environment. This can be achieved by developing more efficient dyeing processes that use less water, reducing the concentration of dyes in the wastewater, and implementing water reuse strategies.

Tea, derived from the dried and processed leaves of the *Camellia sinensis* plant, is the most widely consumed non-alcoholic beverage worldwide, prized for its aromatic fragrance and refreshing taste [17] and is considered a staple of many cultures according to the International Tea Committee's report. The major contributors to tea production in India are the northeastern states of Assam and West Bengal [18–22]. The production of tea involves the extraction of tea leaves using hot water, which generates a significant amount of spent tea leaves as a waste byproduct. As a result, discovering a use for this waste material has become a pressing concern for tea manufacturers. The abundance of tea waste has prompted researchers to evaluate its potential use as an adsorbent. The conversion of tea waste into adsorbent material is not only economically feasible due to its ready availability, but also offers the additional benefit of waste management. Therefore, tea waste-derived adsorbents represent a promising solution that is environmentally sustainable and economically viable [20,23].

The utilisation of tea waste ash shows promise as an excellent adsorbent material for water treatment applications. Ash is a carbonaceous material obtained from the pyrolysis of organic substances, including tea waste. Ash's porous nature makes it an efficient adsorbent, capable of removing impurities from water (as depicted in Figure 2). Compared with other adsorbents, tea waste ash offers several noteworthy benefits. First and foremost, it is a cost-effective adsorbent, as it can be obtained from a readily available waste material such as agricultural waste and requires a straightforward production process. Moreover, the use of tea waste ash in water treatment applications can help manage the accumulation of waste in landfills, thereby supporting a sustainable approach [24]. The use of tea waste ash for the removal of malachite green from water is a promising approach due to its adsorption properties. Tea waste ash has a high surface area and pore volume, which allows it to adsorb malachite green from water effectively. It is an easily available and low-cost adsorbent that can be found in every household. Several studies have reported the use of tea waste-derived ash and other biomass-based adsorbents for dye removal from aqueous media. However, most of these adsorbents require chemical activation, surface modification, or

incorporation of nanomaterials to achieve high adsorption performance, which increases production cost, processing complexity, and environmental concerns. Furthermore, limited studies have explored the direct utilisation of Camellia sinensis waste ash prepared by simple calcination without any chemical treatment, particularly for the removal of Malachite Green dye. This represents an important research gap in developing low-cost, sustainable, and readily scalable adsorbents from tea waste. Therefore, the present study investigates, for the first time, the adsorption performance of unmodified Camellia sinensis ash as a non-conventional adsorbent for Malachite Green removal. Unlike many chemically modified biomass-derived adsorbents reported in the literature, the proposed adsorbent is prepared through a simple calcination process without the use of activating agents or hazardous chemicals [25–27]. Despite its simple preparation, it exhibited excellent dye removal efficiency and favourable adsorption kinetics, demonstrating that waste tea ash can serve as an efficient, economical, and environmentally benign adsorbent for wastewater treatment. The findings highlight a sustainable approach to valorising tea waste while providing a practical alternative to chemically modified biomass adsorbents.

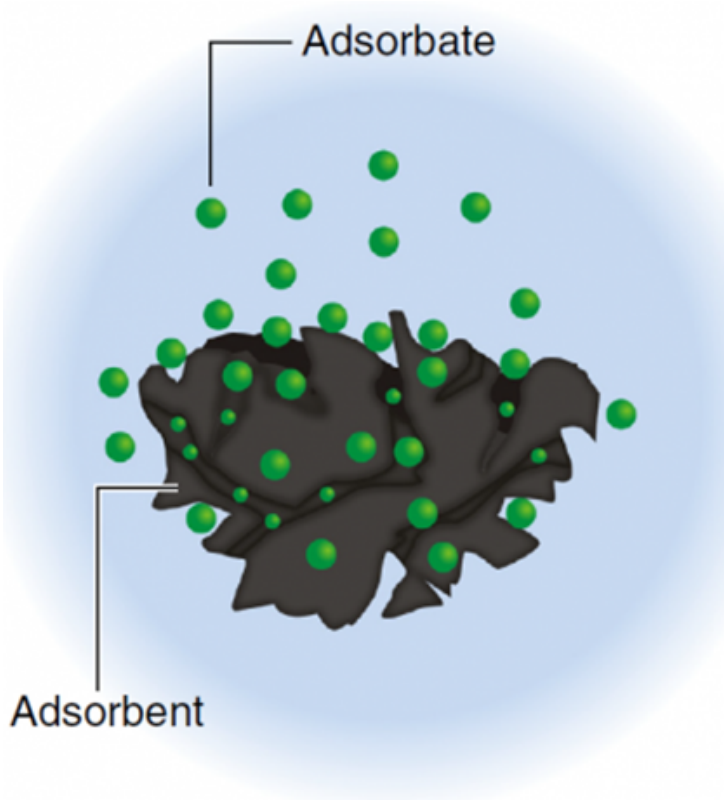

Figure 2. Adsorption process demonstration.

2. Methods and Materials

Tata tea waste was collected from a retail outlet in Koni Bilaspur and thoroughly washed using distilled water. It was then air-dried to remove excess moisture and subjected to a pulverization process to generate a fine powder. The powder was incorporated into a muffle furnace at 500 °C for 5 h, where the resultant ash was allowed to cool at room temperature for 24 h before subsequent tests. After calcination, we obtained 5 g of tea ash from 100 g of oven-dried tea waste. The efficiency of the tea powder ash was evaluated based on dye solutions of malachite green. The findings revealed that the tea powder ash demonstrated a remarkable ability to remove malachite green dye within a short duration of contact time. Further testing was conducted using different concentrations of the malachite green dye, ranging from 10 mg/L to 40 mg/L.

2.1. Adsorption Experimental Design

To assess the effectiveness of tea powder ash in eliminating MG dye, several parameters, such as temperature, contact time, adsorbent dosage, pH levels, and the initial dye concentration, were evaluated in a batch. The process began by creating a stock solution of MG dye. Various concentrations of the dye solution were subjected to spectral readings, with the results demonstrating a linear relationship between the absorbance and the dye concentration.

The effectiveness percentage of tea powder ash was calculated by introducing 10 mg of the adsorbent into a 10 mL solution of MG dye and determining the remaining dye concentration via absorbance measurements

conducted at λ_{max} = 617 nm. The adsorption capacity of tea powder ash for MG dye, defined as the quantity of dye (in mg) adsorbed per gram of adsorbent (Q_e), was calculated utilizing appropriate equations.

$$\text{Dye Removal (\%)} = \left(1 - \frac{C_e}{C_o}\right) \times 100 \quad (1)$$

$$Q_t = \frac{(C_o - C_t)v}{m} \quad (2)$$

$$Q_e = \frac{(C_o - C_e)v}{m} \quad (3)$$

In these equations, C_e (mg/L) and C_t (mg/L) represent the initial and final concentrations of dye, respectively. V (L) represents the initial volume of the dye solution, and m (mg) represents the weight of adsorbents [25].

2.2. Study of Adsorption Isotherm

The adsorbent-dye interaction behavior and distribution of MG dye molecules between the solid and liquid phases were assessed using three distinct adsorption isotherm models -Freundlich, Langmuir, and Temkin. Implementing these adsorption isotherm models provides an opportunity to deepen the understanding of adsorption phenomena and express complex mechanisms in quantifiable variables. The nonlinear Freundlich model characterizes a form of physical adsorption in multiple layers, with relatively weak bonds between the absorbent and adsorbate (multilayer). Additionally, the Freundlich isotherm provides insight into the linearity of the relationship between the adsorbate solution and adsorption process, which can fall into several categories of linear and nonlinear adsorption chemical interaction adsorption and physical interaction adsorption [28].

According to the nonlinear Langmuir isotherm model, a monolayer of adsorbate on the adsorbent surface defines the maximum adsorbent capacity. This suggests that the most significant quantity of adsorbate that can be adsorbed onto the adsorbent material is the point at which a monolayer is formed.

The linear Temkin model evaluates the interaction and affinity between the adsorbent and adsorbate, ensuring the binding energy is uniformly distributed across the surface.

To facilitate comprehension of these models, the graph is plotted between Ce and qe and fitted according to the nonlinear equations of Freundlich isotherm and Langmuir isotherm in (Equations (4) and (5)), respectively, and the linear Temkin equation according to Equation (6).

Freundlich adsorption isotherm:

$$q_e = K_f(C_e^{1/n}) \quad (4)$$

Langmuir adsorption isotherm:

$$q_{e=\frac{q_m k_L C_e}{1+K_L C_e}} \quad (5)$$

Temkin adsorption isotherm:

$$Q_e = \frac{RT}{b_T} lnC_e + \frac{RT}{b_T} lnK_T \quad (6)$$

The amount of adsorbate absorbed at equilibrium by an adsorbent is Qe (mg/g) based on the equilibrium concentration of the dye solution, Ce (mg/L). These parameters are defined by empirical constants, such as K_f and n for the Freundlich isotherm, K_L and Q_L for the Langmuir isotherm, and b_T and K_T for the Temkin isotherm. These constants consider all the variables that impact the adsorption process [29–32].

R = Gas constant and value of 8.314 J/mol K,

T = Temperature in Kelvin. In the Freundlich isotherm,

K_f and 1/n = Adsorption Capacity and Surface Heterogeneity. For the Langmuir isotherm,

Q_L and K_L = Adsorption Capacity and Energy Adsorption. For the Temkin isotherm,

K_T = Associated with the Equilibrium Binding Energy

b_T = Heat of adsorption.

2.3. Adsorption Kinetics Study

The subject of adsorption kinetics research is how quickly absorbate is either absorbed or released at the interface between a solid substance and an aqueous solution. We can compare the goodness of fit index to identify the best model after conducting a variety of linear or non-linear analysis to comprehend how the process operates [33,34].

Pseudo-first order (Largergren model)

$$\log(Q_e - Q_t) = \log(Q_e) - \frac{k_1}{2.303}t \tag{7}$$

Pseudo second order

$$\frac{t}{Q_t} = \frac{t}{Q_e} + \frac{1}{k_2 Q_e^2} \tag{8}$$

Inter-particle-diffusion kinetics

$$Q_t = k_i t^{1/2} + C \tag{9}$$

where Q_e (mg g^{-1}) and Q_t (mg g^{-1}) are values of the adsorbed adsorbate at equilibrium and at time t, respectively, and k_1 (min^{-1}) is the pseudo-first-order rate constant and k_2 (g/mg min) is the pseudo-second-order rate constant k_i stands for interparticle diffusion rate constant.

2.4. Thermodynamics Study

The thermodynamic study [35] of adsorption involves the analysis of the energy changes that occur when a substance is adsorbed onto a surface. Free energy (G), enthalpy (H) and entropy (S) for the adsorption of the dye were calculated by using Equations (10) and (11).

$$\frac{Q_e}{C_e} = \frac{\Delta S}{R} - \frac{\Delta H}{RT} \tag{10}$$

$$\Delta G = \Delta H - T\Delta S \tag{11}$$

3. Result and Discussion

3.1. Characterisation of Camellia Sinensis Ash (Tea Powder Ash)

The Fourier transform infrared spectrum presented in the accompanying Figure 3 depicts the characteristic peaks of *Camellia sinensis* ash. Broad peaks are observed in the range of 2900–3700 cm^{-1}. The peak observed at 2350 cm^{-1} indicates the stretching vibrations of O=C=O (Carboxyl) groups, The peaks observed at 1405 cm^{-1} are assigned to the asymmetric and symmetric stretching of the carboxylate groups [33]. Additionally, the band at 1039 cm^{-1} is assigned to the (C-H) vibration of the aromatic ring. Broad Peak at 3405 cm^{-1} is characteristic of the stretching vibrations of -OH groups, likely associated with hydroxyl groups on the adsorbent surface [32].

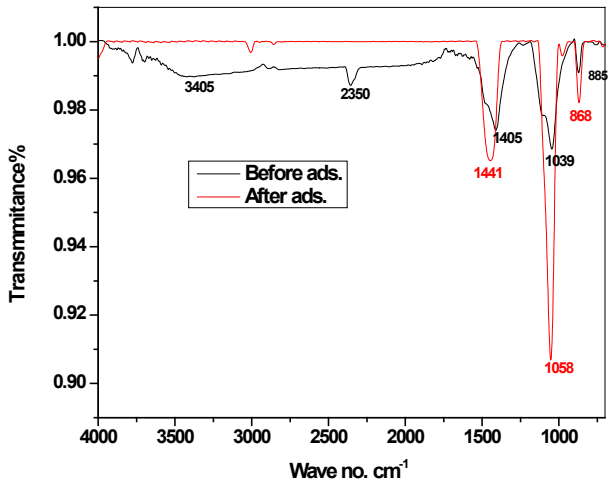

Figure 3. FT−IR spectrum of *Camellia sinensis* ash.

The crystalline structure of *Camellia Sinensis* ash was analysed by X-ray diffraction. X-ray diffraction of before and after adsorption of *Camellia Sinensis* ash is shown in Figure 4. The tea ash's nanocrystalline structure is confirmed by the computed average crystallite size of 34 nm. The thermal breakdown of organic components and the subsequent crystallisation of naturally occurring inorganic minerals during calcination at 500 °C are responsible for the production of nanosized crystallites. Potassium, calcium, silica, magnesium, and phosphorus found in tea leaves are the main sources of the crystalline phases. The existence of a significant calcium-rich crystalline phase, most likely calcite, is indicated by the prominent diffraction peak at about 2θ = 29°. Various diffraction peaks correspond to various silicates and mineral oxides. Because it offers a larger specific surface area and more accessible adsorption sites, the nanocrystalline structure with an average crystallite size of 34 nm is beneficial for adsorption applications, improving the interaction between the adsorbent and adsorbate.

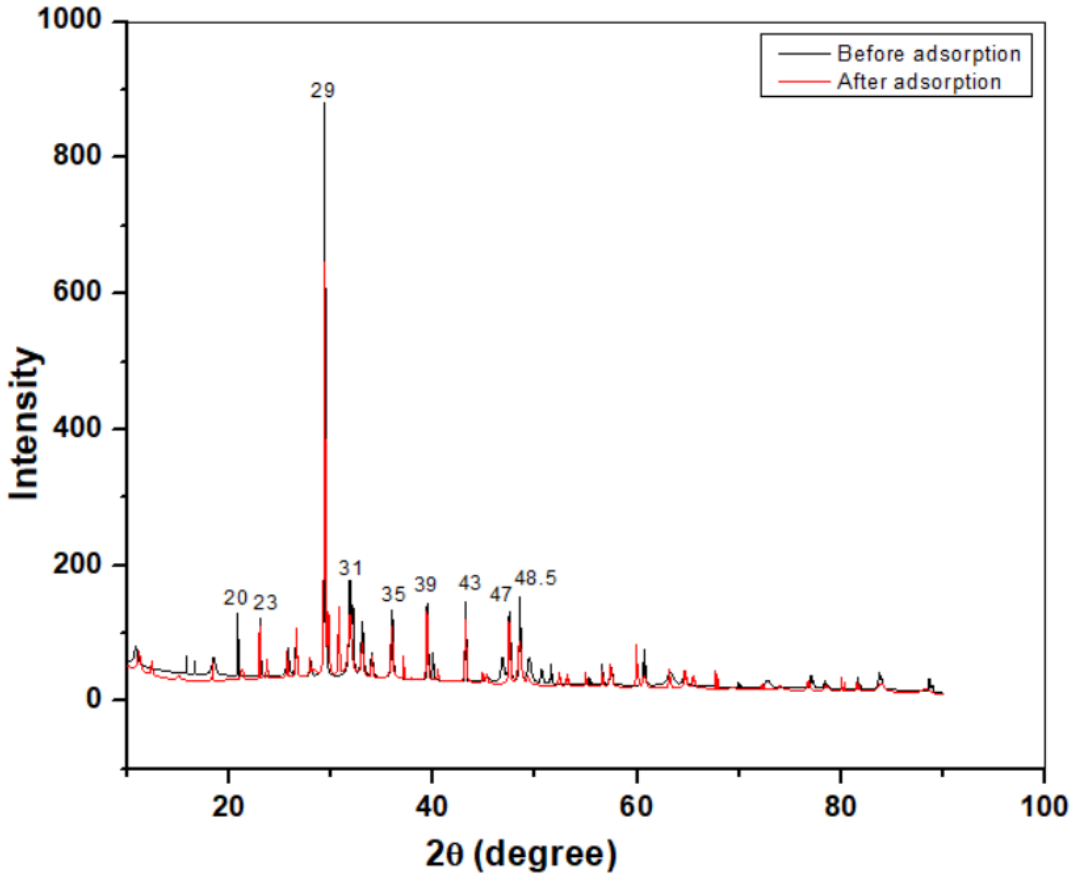

Figure 4. X-ray diffraction of *Camellia sinensis* ash.

The Brunauer–Emmett–Teller (BET) method was employed to determine the specific surface area and pore characteristics of the adsorbent. Based on the BET isotherm plot (Figure 5), the adsorbent exhibited a mesoporous structure, as evidenced by the hysteresis loop and average pore radius. The presence of mesopores provides accessible sites for the adsorption of dye molecules of different sizes. The BET surface area of the pristine adsorbent was found to be 42.626 m^2/g, which decreased to 20.96 m^2/g after adsorption of MG dye. Similarly, the total pore volume decreased from 0.214 to 0.175 cm^3/g, while the average pore radius of 15.277 Å confirmed the mesoporous nature of the adsorbent. The reduction in surface area and pore volume after MG adsorption can be attributed to the occupation and partial blockage of the accessible pores by dye molecules, which restricts the accessibility of nitrogen molecules during BET analysis [36]. In addition, interactions between MG molecules and the adsorbent surface may lead to pore filling and/or aggregation of adsorbent particles, resulting in a decrease in the accessible surface area and pore volume. These changes further support the successful adsorption of MG within the porous structure of the adsorbents [37].

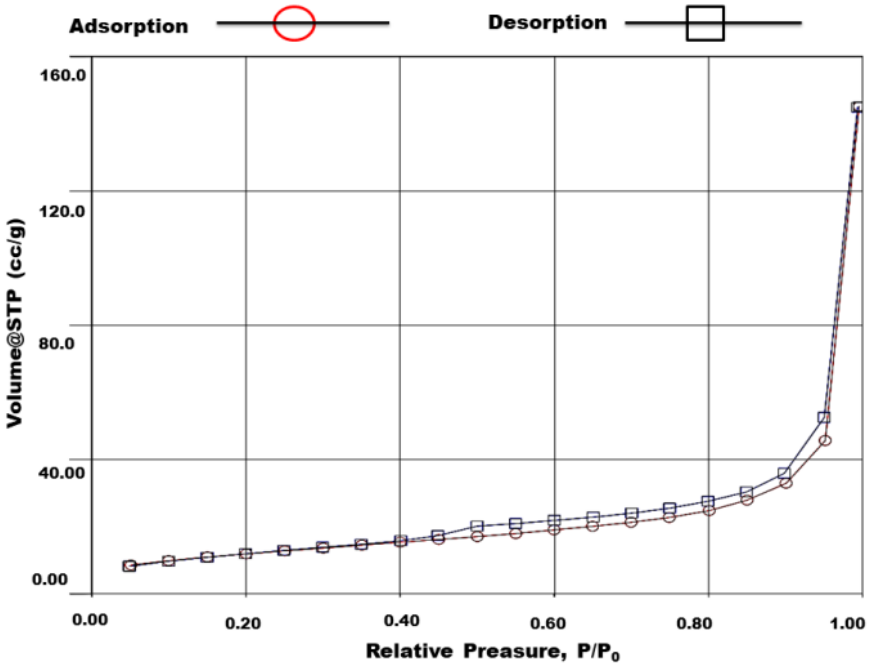

Figure 5. BET plot of the N_2 adsorption−desorption isotherm.

SEM image analysis of *Camellia sinensis* ash provides comprehensive insights into its structure and potential applications. Such analyses can guide the development of sustainable practices by utilizing agricultural waste effectively and contributing to circular economy practices. The SEM images (Figure 6) provide strong evidence for the successful adsorption of Malachite Green dye onto *Camellia sinensis* ash (tea waste ash). The significant change in surface morphology, characterized by increased roughness and the presence of fine particles, indicates that the dye molecules have interacted with the ash surface and become attached. This conclusion aligns with the observed decrease in dye concentration in the solution after the adsorption process.

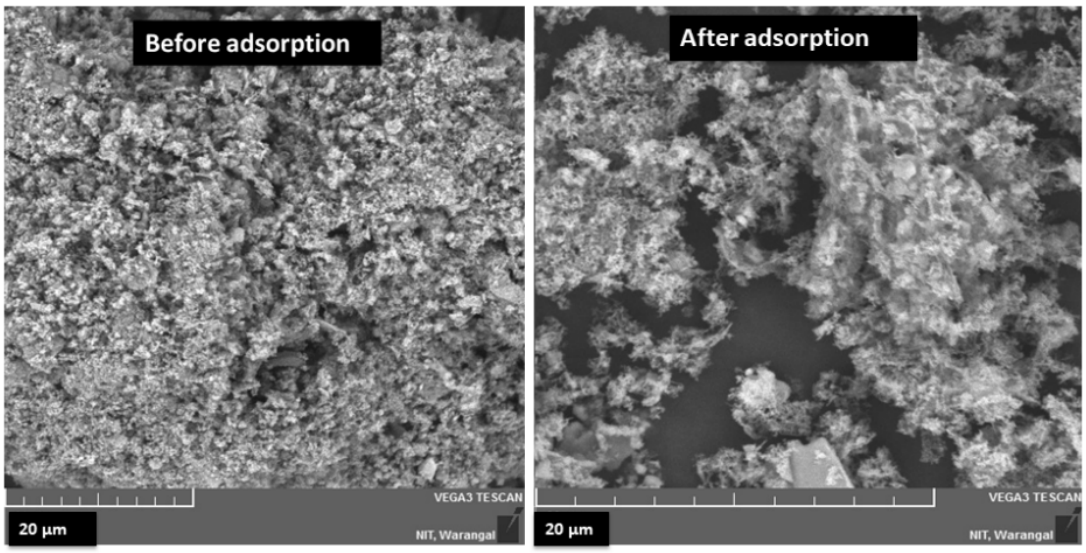

Figure 6. SEM image of *Camellia sinensis* ash before and after adsorption.

3.2. Effect of Initial Dye Concentrations

To investigate the influence of initial dye concentration on the adsorption efficiency of the adsorbent. An adsorbent mass of 10 g was utilised, and the dye concentrations were varied between 5 mg/L and 25 mg/L at standard temperature. It was observed that the removal efficiency of the adsorbent was relatively low for lower dye concentrations, but increased gradually as the contact time increased. The findings were further illustrated in the accompanying Figure 7. After 240 min of contact time, a maximum removal efficiency of 95.87% was achieved for a dye concentration of 25 mg/L. The observed increase in adsorption capacity can be attributed to a greater

mass gradient between the dye solution and the adsorbent when the initial dye concentration is higher [38]. However, once the adsorbent reaches its maximum saturation capacity, adsorption is limited, and no further dye removal can be obtained.

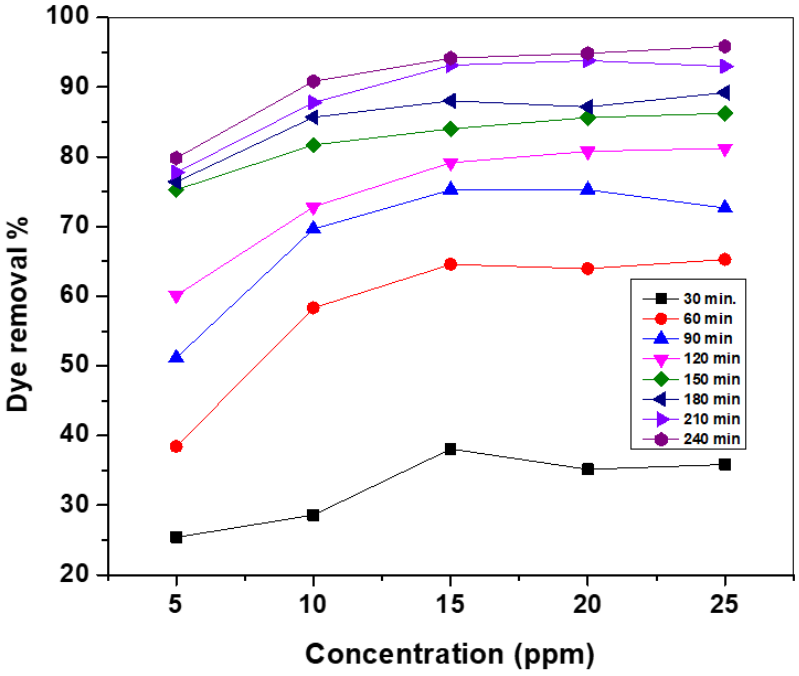

Figure 7. Effect of initial dye concentration of MG dye.

3.3. Effect of Adsorbent Dose

The impact of varying adsorbent dosage on the adsorption efficiency of MG dye was evaluated by altering the adsorbent quantity in the range of 10 mg to 50 mg, while keeping the dye concentration constant at 20 mg/L. The findings, as depicted in the accompanying Figure 8, demonstrate that the removal percentage of MG dye increases proportionately with an increase in the quantity of adsorbent used. The observed increase in MG dye adsorption can be attributed to an increase in the surface area of the adsorbent and the number of active sites, which become available with an increase in the adsorbent dosage [28].

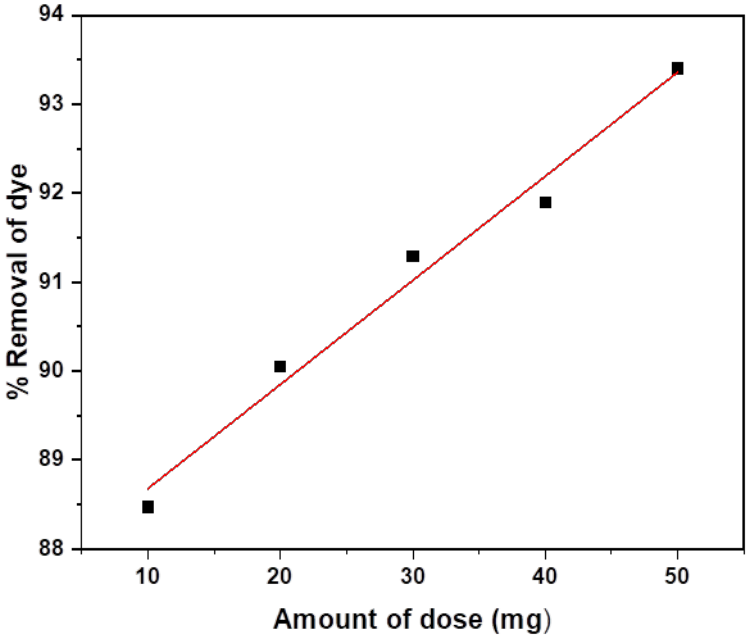

Figure 8. Effect of adsorbent dose on removal of MG Dye by using Tea Powder Ash as an adsorbent.

3.4. Effect of pH

The effect of pH on the adsorption of Malachite Green (MG) dye onto *Camellia sinensis* ash was investigated over the pH range of 3–10 using 5 mg of adsorbent and 5 mL of a 20 mg/L dye solution. The results (Figure 9) showed that the adsorption of MG increased gradually with increasing pH and reached its maximum under alkaline conditions. This behaviour can be explained based on the point of zero charge (pHpzc) of the adsorbent, which was determined to be approximately 9 (Figure 10). At pH values below the pHpzc, the adsorbent surface is predominantly positively charged due to protonation of the surface functional groups. Since Malachite Green is a cationic dye, electrostatic repulsion between the positively charged adsorbent surface and dye molecules reduces the adsorption capacity. As the solution pH approaches the pHpzc, the positive surface charge decreases, resulting in reduced electrostatic repulsion and improved dye adsorption. At pH values above the pHpzc, the adsorbent surface becomes negatively charged because of deprotonation of the surface functional groups. This promotes strong electrostatic attraction between the negatively charged surface and the positively charged MG molecules, leading to the highest adsorption efficiency. In addition to electrostatic interactions, pore diffusion and surface functional groups may also contribute to the adsorption process [36].

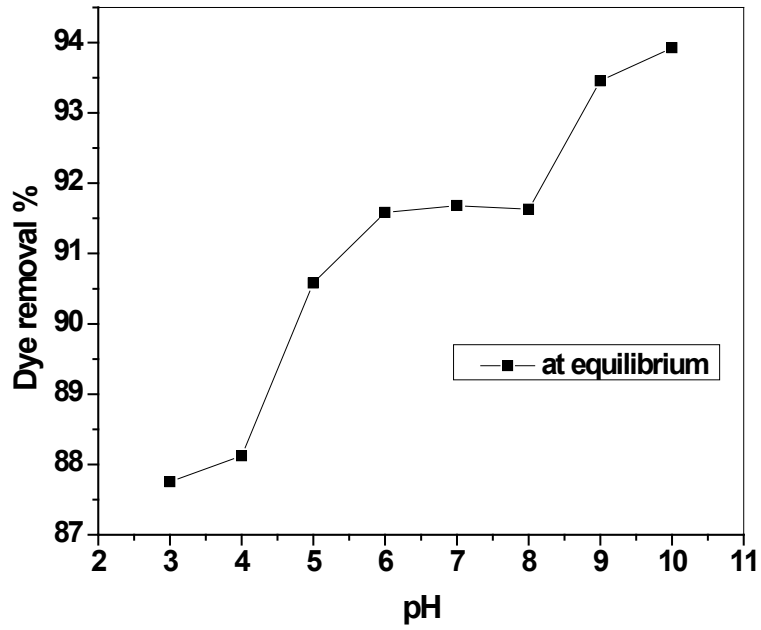

Figure 9. Effect of pH on removal of MG Dye by using *Camellia sinensis* ash (Tea Powder Ash) as an adsorbent.

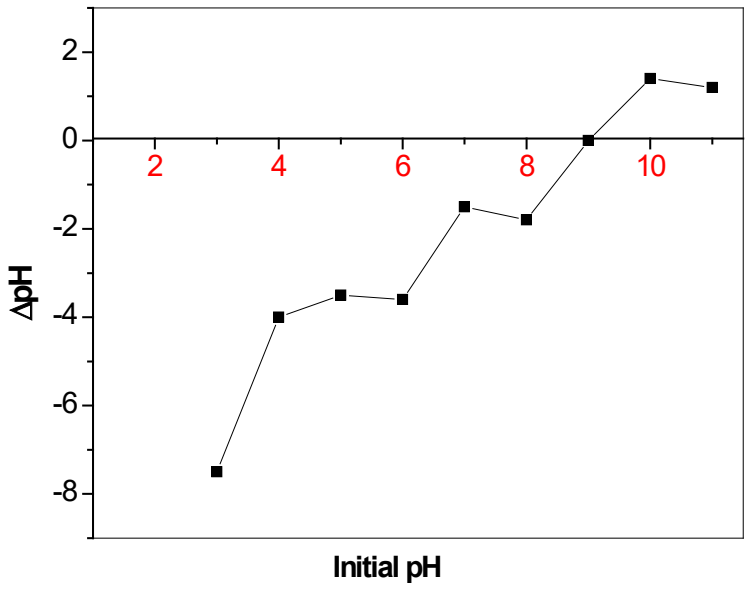

Figure 10. Point zero charge of *Camellia sinensis* ash (Tea Powder Ash).

3.5. Effect of Temperature

The impact of temperature on the adsorption process was investigated, and it was found to play a significant role in the efficiency of adsorption. To explore this phenomenon, adsorption experiments were conducted for a duration of 3 h at varying temperatures, including 40 °C, 45 °C, 50 °C, and 55 °C. In these experiments, 10 mg of adsorbent was subjected to 5 mL of 10 mg/L dye for adsorption. The accompanying Figure 11 illustrates that the amount of dye removed showed a slight increase with temperature increments. The observed trend can be attributed to the effect of temperature on the equilibrium capacity of the adsorbent and adsorbate [39]. Factors such as a decrease in solution viscosity and an increase in the diffusion rates of dye molecules over external barriers could also contribute to the observed trend [40].

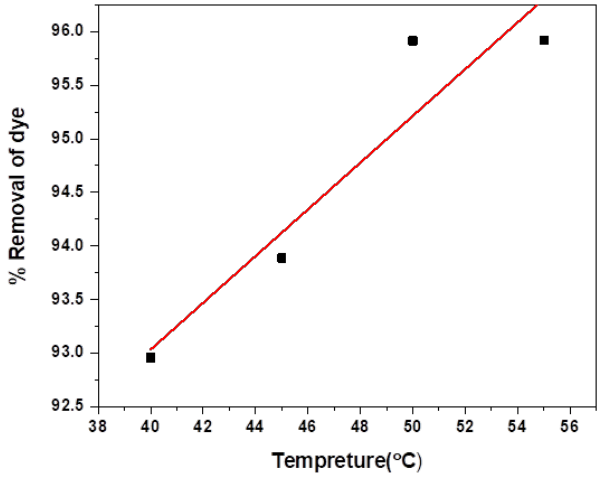

Figure 11. Effect of temperature on removal of MG Dye by using Tea Powder ash as an adsorbent.

3.6. Column Procedure for Removal of MG dye

To assess the practical use of *Camellia sinensis* ash as an adsorbent, we conducted a column experiment to test its ability to remove Malachite Green (MG) dye. During the static bed trial, we observed a complex breakthrough curve, which is a graph showing how the dye was removed over time (as illustrated in the accompanying Figure 12). Initially, there were many available spots on the surface of the ash for the dye to attach, which resulted in complete removal of the dye from the solution. At this stage, the ratio of the concentration of dye in the column (C_t) to the initial concentration (C_0) was zero. As time passed, we noticed a different trend: the dye concentration began to increase slightly in the effluent. This gradual increase continued over the duration of the experiment, leading to the formation of the breakthrough curve. We calculated the area under this curve to be 884.42 cm^2, which reflects the overall performance of the column. We found that the total amount of MG dye adsorbed per gram of the adsorbent was 75.02 mg/g. [41–43]

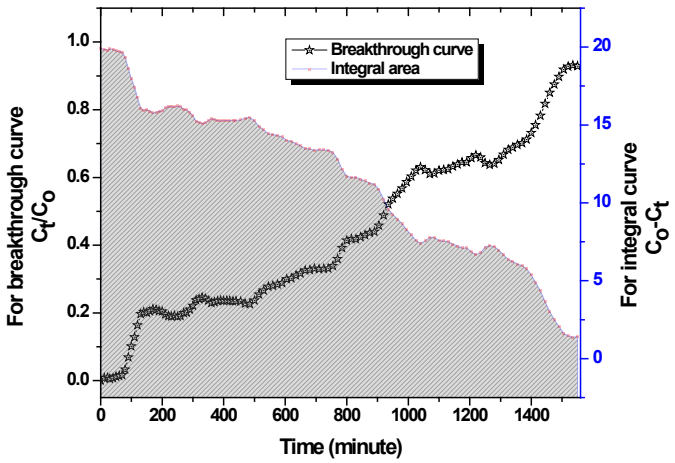

Figure 12. Breakthrough curve (line, left vertical axis) and integral area (shaded, right vertical axis) of MG on *Camellia sinensis* in a fixed bed column experiment.

3.7. Study of Adsorption Isotherm

The equilibrium isotherm value is a widely accepted approach for presenting adsorption data, which involves depicting the quantity of adsorbate removed per unit adsorbent in relation to the solid phase concentration of the sorbent and the concentration of the adsorbate in the liquid phase. The development and improvement of an adsorption system that is utilized in eliminating dyes from aqueous solutions largely depend on the accuracy of the equilibrium isotherm value. Selecting the most fitting correlation for the equilibrium curve is crucial when analysing the interaction between adsorbents and dyes. Several adsorption isotherms are available to investigate this interaction, and in this study, the Freundlich, Langmuir, and Temkin isotherm models were employed to analyse the interface between MG dye and tea powder ash. The results and parameters of the adsorption isotherm fits are presented in Figure 13 and Table 1. The relationship between the remaining dye content and the three adsorption isotherms was evaluated, and it was determined that the Temkin isotherm had the most suitable fit for this study, as determined by the coefficient of determination (R^2). The R^2 value is used in adsorption to represent the proportion of dependent variable variance that can be predicted from the independent variable. The results of this experiment indicate that the linear Temkin adsorption isotherm was the most suitable, with an R^2 value of 0.95. In the Freundlich isotherm, the intercept value is K_f, which was calculated to be 33.24, while the slope is 1/n, with n equal to 0.007. The Langmuir isotherm provided useful information regarding the extent of interaction between the adsorbent and adsorbate. From the findings, the maximum value is identified as 36.35 mg/g, and K_L is determined to be 0.53. The Temkin model is designed to account for the interaction between the adsorbate and the adsorbing species. It assumes that there is a uniform distribution of binding energies, and that the heat of adsorption of each molecule in the layer decreases linearly with temperature instead of logarithmically with coverage. Another important parameter in the Temkin model is the constant C, which provides valuable information about the thickness of the bound layer and its resistance to external mass transfer [44,45]. The Langmuir isotherm showed a relatively low correlation coefficient ($R^2 = 0.60$), indicating that the adsorption of Malachite Green onto tea waste ash does not follow ideal monolayer adsorption on a homogeneous surface. In contrast, the Freundlich ($R^2 = 0.93$) and Temkin ($R^2 = 0.95$) models provided a much better fit to the experimental data, suggesting that the adsorbent surface is heterogeneous and contains adsorption sites with different binding energies. The superior agreement with the Temkin model further indicates that adsorbate–adsorbent interactions influence the adsorption process and that the heat of adsorption decreases progressively as surface coverage increases. Therefore, the adsorption of Malachite Green onto tea waste ash is better described as occurring on a heterogeneous surface through multiple adsorption sites rather than by the assumptions of the Langmuir model.

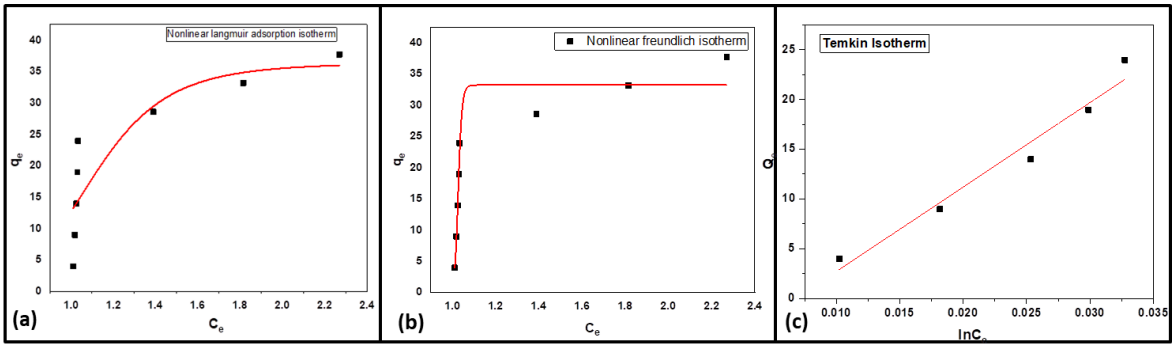

Figure 13. The plot of adsorption isotherm (**a**) Langmuir isotherm (nonlinear) (**b**) Freundlich isotherm (nonlinear) and (**c**) Temkin isotherm (linear).

Table 1. Adsorption isotherm parameters.

Freundlich Isotherm			Langmuir Isotherm			Temkin Isotherm		
n	K_f	R^2	Q_{max}	K_L	R^2	b_T	K_T	R^2
0.007	33.24	0.93	36.35	0.53	0.6	2.97	0.99	0.95

3.8. Kinetic Study of Adsorption

The adsorption behavior of tea powder ash materials can be attributed to the active groups and bonds present on their surface. A kinetic analysis of the adsorption process is essential in determining the adsorption efficiency since aqueous phase adsorption exhibits rapid kinetics. In this study, various kinetic models, including inter-particle diffusion, pseudo-first order, and pseudo-second-order methods, were employed to analyze the collected

data. Initially, the Lagergen pseudo-first-order model was employed to evaluate the kinetics data in the current system. The collected kinetic data was then examined using linear kinetics models. The correlation coefficient model was found to have the highest R^2 value, indicating that it provides the best description of the kinetics and measures the degree of agreement between the experimental data and the chosen kinetic model. The fitting plots for all the examined kinetic models are presented in Figure 14 and the corresponding values are summarized in Table 2. Based on the results, it was concluded that the first order kinetic model exhibited the best fit with a regression coefficient of 0.98. For the pseudo-second order and interparticle diffusion kinetics models, the correlation coefficients were 0.93 and 0.79, respectively. The data indicated that the adsorption process is primarily physical, as it involves weak attractions between the MG molecules and the adsorbent. The experimental q_e value, determined using the pseudo-first order kinetics model, was 23.966 mg/g, which was similar to the calculated data. Additionally, compared to the pseudo-second-order model's prediction of 28.653 mg g^{-1}, the computed equilibrium adsorption capacity (Qe) from the pseudo-first-order model (22.76 mg g^{-1}) is closer to the experimental adsorption capacity. This further demonstrates that the pseudo-first-order model offers the best explanation of the adsorption kinetics of Malachite Green onto tea waste ash, along with its better correlation coefficient [46–49].

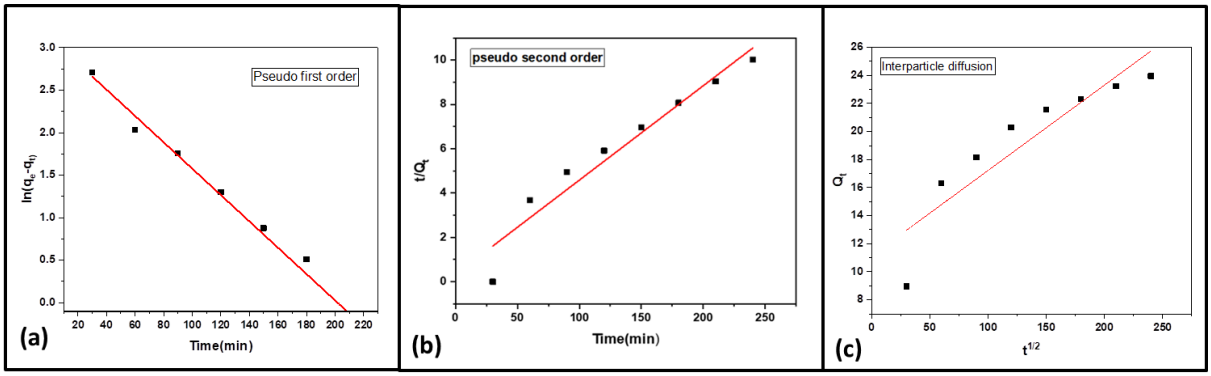

Figure 14. The linear plot of (**a**) Pseudo-first-order kinetic model, (**b**) pseudo-second-order kinetic model, (**c**) intraparticle diffusion model.

Table 2. Values of kinetics parameters.

Q_e (mg/g)	Pseudo First Order			Pseudo Second Order			Intraparticle		
	Q_e	K_1	R^2	Q_e	K_2	R^2	K_I	C	R^2
23.966	22.760	0.0357	0.982	28.653	0.005	0.93877	0.061	11.140	0.797

3.9. Thermodynamic Study

The kinetics of the adsorption process were found to be faster at higher temperatures, indicating the significant impact of temperature on the process. The thermodynamic parameters, such as ΔG, ΔH, and ΔS, were evaluated using Equations (10) and (11) based on mathematical formulas. The values of ΔH and ΔS were obtained from the slope (ΔH/R) and intercept (ΔS/R) of the linear plot of $\ln(Q_e/mC_e)$ versus 1/T (see Figure 15). The calculated thermodynamic parameter values are reported in Table 3. It was observed that a negative value of ΔG was obtained for each of the four temperatures, suggesting that the adsorption process is spontaneous. The negative values of ΔG indicate that the adsorption process is spontaneous, and the decrease in ΔG (i.e., becoming more negative) with increasing temperature demonstrates that the adsorption becomes more thermodynamically favourable at higher temperatures. This observation is consistent with the positive value of ΔH, confirming the endothermic nature of the adsorption process [50]. The adsorbent/adsorbate interaction is more random when ΔH and ΔS values are positive [51]. Since the value of ΔH is less than 40 kJ/mol the adsorption is physisorption in nature [52].

Table 3. Thermodynamic parameters.

ΔH(kJ/mol)	ΔS(kJ/mol/K)	ΔG(kJ/mol) at Temperatures				
		308.15 K	313.15 K	318.15 K	323.15 K	328.15 K
36.879	0.12005	−0.114	−0.804	−1.4049	−2.005	−2.605

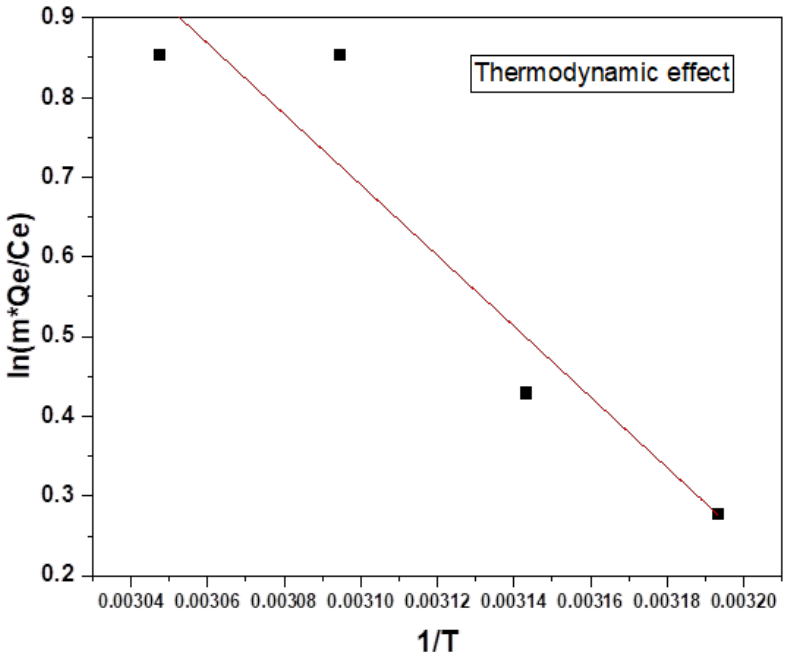

Figure 15. Linear Plot of ln ($Q_e m/C_e$) versus 1/T to give thermodynamic parameters.

3.10. Desorption of Adsorbed MG and Reusability of Adsorbent

Adsorbent reusability and sludge management after sorption are the main goals of the desorption experiments. For practical and cost-effective uses, adsorbents must be reusable over several sorption-desorption cycles. The high cost of wastewater purification systems has made adsorbent regeneration and reuse more commercially relevant. Adsorbents are costly for industrial application if they cannot be used again or if their adsorption efficacy is greatly diminished with repeated use. They also cause secondary environmental damage. Therefore, it is necessary to perform desorption research of MG (25 mg/L). According to Figure 16, the adsorbent can remove 53.65% of the MG dye after four consecutive cycles of adsorption–desorption [53,54].

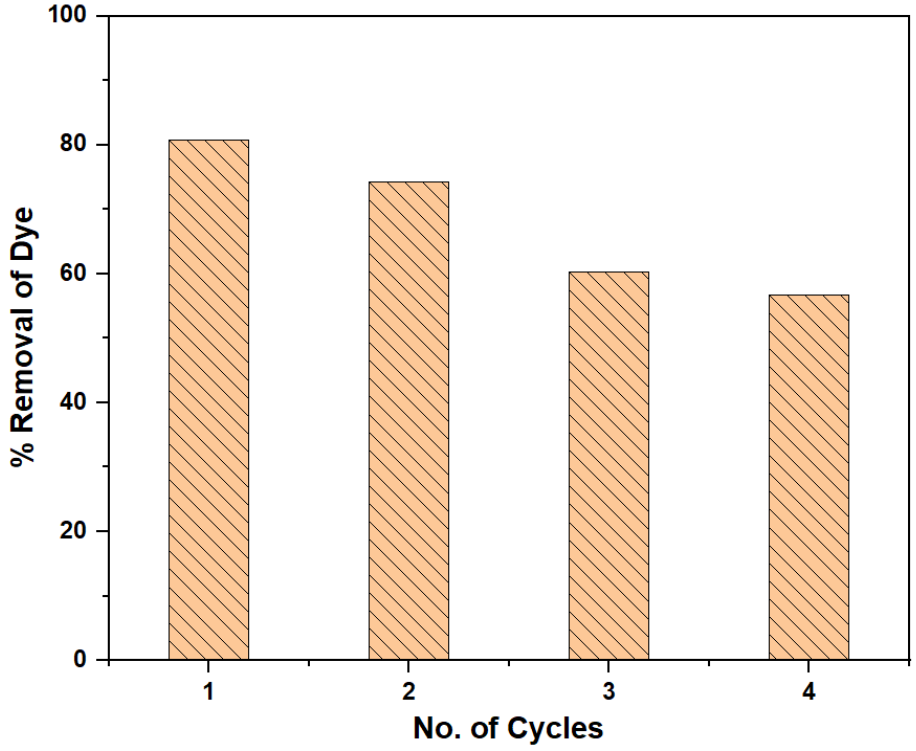

Figure 16. Desorption curve of MG.

3.11. Performance Comparison of the Present Adsorbent with Other Biomass-Based Materials for Malachite Green Removal

The Camellia sinensis ash adsorbent developed in the present study exhibited a malachite green adsorption capacity of 75.02 mg/g (Table 4). Among unmodified/minimally processed plant-based adsorbents, it outperformed willow tree leaves ash (21.44 mg/g), palm leaves ash (62.80 mg/g), Juniperus excelsa cone ash (38.02 mg/g), and water hyacinth ash (102.35 mg/g), while showing comparable or higher capacity than most literature-reported materials without requiring chemical activation or modification. As shown in Table 4, several modified or activated biomass-derived adsorbents exhibit higher adsorption capacities than the present adsorbent. For instance, *Myriophyllum aquaticum* biochar reported an adsorption capacity of 1772.3 mg g^{-1}, which can be attributed to its engineered preparation and enhanced surface characteristics, while activated plantain leaf biochar achieved 266.80 mg g^{-1} following chemical activation. Although these modified adsorbents demonstrate superior adsorption performance, their preparation involves additional processing and chemical activation, increasing production cost and complexity. In contrast, the Camellia sinensis ash used in this study is produced by simple calcination without any chemical modification and still exhibits a competitive adsorption capacity (75.02 mg g^{-1}) together with excellent dye removal efficiency, highlighting its potential as a low-cost, sustainable, and environmentally friendly adsorbent for wastewater treatment [55].

Table 4. Adsorption performance of different unmodified and modified plant-derived adsorbents for malachite green dye removal.

Material Used	Amount of Dye Adsorbed per g Adsorbent (mg/g)	Kinetics Model Followed	Adsorption Isotherm Followed	Reference
Camellia sinensis ash (tea powder ash)	75.02	Pseudo-first-order	Temkin	Present work
Willow tree leaves ash (*Salix alba* L.)	21.244	Pseudo-second-order	Langmuir and Freundlich	[45]
Water lily stem ash (*Nymphaea lotus)*	102.35	Pseudo-first-order	Langmuir	[46]
Palm leaves hydrochar (activated)	62.80	Pseudo-second-order	Langmuir	[47]
Myriophyllum aquaticum ash	1772.3	Pseudo-second-order	Langmuir	[48]
Juniperus Excelsa cone ash (modified)	38.023	Pseudo-second-order	Langmuir	[49]
Mandarin peel ash (with nZVI)	909.09	Pseudo-second-order	Freundlich	[50]
Cassava peel ash (Modified)	282.64	Pseudo-second-order	Langmuir	[51]
Plantain leaf ash (activated)	266.80	Avrami fractional	Redlich-Peterson	[52]

4. Conclusions

In conclusion, our studies show that *Camellia sinensis* ash (tea powder ash) is an effective material for removing Malachite Green (MG) dye from water. We carefully evaluated various factors that influence its adsorptive capacity, including pH, temperature, initial dye concentration, contact time, and the amount of adsorbent used. Notably, at a temperature of 30 °C, the ash was able to remove approximately 95.87% of the MG dye from a 25 mg/L solution. Our findings also revealed that increasing the amount of tea waste ash enhances the dye removal capability. The pH tests indicated that tea ash performs particularly well in alkaline conditions when adsorbing cationic dyes like MG. From our column experiments, we determined that the total amount of MG dye adsorbed was 75.02 mg of dye per gram of adsorbent. The best-fitting model for our adsorption data was the Temkin isotherm, achieving a high correlation coefficient of 0.95. Kinetic analysis indicated that the adsorption process is endothermic, and among the three kinetic models we examined, the pseudo-first-order model provided the best fit. This suggests that the dye adsorption occurs mainly through physisorption, a physical process. Thermodynamic studies further confirmed that the adsorption process occurs favourably and spontaneously at elevated temperatures. Overall, these results suggest that tea powder ash is a cost-effective and efficient adsorbent for the removal of Malachite Green dye from aqueous solutions.

Author Contributions

S.K. (Santosh Kumar), N.R. and S.K. (Sonu Kumar): Analytical methods, experimental work; S.S. and A.V.: Analysis, calculation and writing manuscript, C.A.: conceptualization, supervision, writing, review and editing All authors have read and agreed to the published version of the manuscript.

Funding

S.K. (Santosh Kumar), A.V. and N.R. are thankful to UGC for providing VRET fellowship.

Institutional Review Board Statement

Not applicable.

Informed Consent Statement

Not applicable.

Data Availability Statement

Data will be made available on request.

Conflicts of Interest

The authors declare no conflict of interest.

Use of AI and AI-Assisted Technologies

If AI tools were used please indicate that "During the preparation of this work, the author(s) used [tool name/service] to [description of use]. After using this tool/service, the author(s) reviewed and edited the content as needed and take(s) full responsibility for the content of the published article."

Or state "No AI tools were utilized for this paper."

References

1. Hussain, S.; Salman, M.; Youngblood, J.P.; et al. Enhanced Adsorption of Congo Red Dye by CS/PEG/ZnO Composite Hydrogel: Synthesis, Characterization, and Performance Evaluation. *J. Mol. Liq.* **2024**, *411*, 125704. https://doi.org/10.1016/j.molliq.2024.125704.
2. Dubey, S.K.; Yadav, R.; Chaturvedi, R.K.; et al. Contamination of Ground Water as a Consequence of Land Disposal of Dye Waste Mixed Sewage Effluents: A Case Study of Panipat District of Haryana, India. *Bull. Environ. Contam. Toxicol.* **2010**, *85*, 295–300. https://doi.org/10.1007/s00128-010-0073-2.
3. Soni, S.; Rai, N.; Bajpai, P.K.; et al. Enhanced Sequestration of an Acidic Dye on Novel Bimetallic Metal-Organic Framework. *J. Dispers. Sci. Technol.* **2022**, *45*, 107–116. https://doi.org/10.1080/01932691.2022.2135521.
4. Tkaczyk, A.; Mitrowska, K.; Posyniak, A. Synthetic Organic Dyes as Contaminants of the Aquatic Environment and Their Implications for Ecosystems: A Review. *Sci. Total Environ.* **2020**, *717*, 137222. https://doi.org/10.1016/j.scitotenv.2020.137222.
5. Pillay, T.V.R. *Aquaculture and the Environment*; Fishing News Books: Oxford, UK, 1992; pp. 235–244.
6. Arora, C.; Kumar, P.; Soni, S.; et al. Efficient Removal of Malachite Green Dye from Aqueous Solution Using Curcuma caesia Based Activated Carbon. *Desalination Water Treat.* **2020**, *195*, 341–352. https://doi.org/10.5004/dwt.2020.25897.
7. Sirach, R.; Dave, P.N. Glutaraldehyde crosslinked chitosan-β-cyclodextrin/ZnO composite for the effective adsorption of Congo red anionic dye: A glimpse into adsorption performance and ANN modeling. *Carbohydr. Polym. Technol. Appl.* **2025**, *10*, 100835.
8. Méndez, A.; Barriga, S.; Saa, A.; et al. Removal of malachite green by adsorbents from paper industry waste materials. *J. Therm. Anal. Calorim.* **2010**, *99*, 993–998. https://doi.org/10.1007/s10973-010-0681-4.
9. Srivastava, S.; Sinha, R.; Roy, D. Toxicological Effects of Malachite Green. *Aquat. Toxicol.* **2004**, *66*, 319–329. https://doi.org/10.1016/j.aquatox.2003.09.008.
10. Fessard, V.; Godard, T.; Huet, S.; et al. Mutagenicity of Malachite Green and Leucomalachite Green in in Vitro Tests. *J. Appl. Toxicol.* **1999**, *19*, 421–430. https://doi.org/10.1002/(sici)1099-1263(199911/12)19:6<421::aid-jat595>3.0.co;2-6.
11. Gerundo, N.; Alderman, D.J.; Clifton-Hadley, R.S.; et al. Pathological effects of repeated doses of malachite green: a preliminary study. *J. Fish Dis.* **1991**, *14*, 521–532. https://doi.org/10.1111/j.1365-2761.1991.tb00607.x.
12. Mittelstaedt, R.A.; Mei, N.; Webb, P.J.; et al. Genotoxicity of Malachite Green and Leucomalachite Green in Female Big Blue B6C3F1 Mice. *Mutat. Res. Genet. Toxicol. Env. Mutagen.* **2004**, *561*, 127–138. https://doi.org/10.1016/j.mrgentox.2004.04.003.
13. Arora, C.; Sahu, D.; Bharti, D.; et al. Adsorption of hazardous dye crystal violet from industrial waste using low-cost adsorbent Chenopodium album. *Desalination Water Treat.* **2019**, *167*, 324–332. https://doi.org/10.5004/dwt.2019.24595.
14. Cevallos-Mendoza, J.; Amorim, C.G.; Rodríguez-Díaz, J.M.; et al. Removal of Contaminants from Water by Membrane Filtration: A Review. *Membranes* **2022**, *12*, 570. https://doi.org/10.3390/membranes12060570.

15. Yang, H.; Zhang, G.; Chen, X.; et al. Quaternized fenugreek gum grafted poly(acrylamide-co-methacryloxyethyltrimethyl ammonium chloride) novel composite hydrogel for efficient removal of Congo red dye. *Int. J. Biol. Macromol.* **2025**, *320*, 146090. https://doi.org/10.1016/j.ijbiomac.2025.146090.
16. Singh, A.; Pal, D.B.; Mohammad, A.; et al. Biological remediation technologies for dyes and heavy metals in wastewater treatment: New insight. *Bioresour. Technol.* **2022**, *343*, 126154. https://doi.org/10.1016/j.biortech.2021.126154.
17. Parmar, N.; Rawat, M.; Kumar, J.V. Camellia sinensis (Green Tea): A Review. *Glob. J. Pharmacol.* **2012**, *6*, 52–59.
18. Jabeen, H.; Shaukat, S.; Abd Ur Rahman, H.M. Deep eutectic solvent mediated synthesis of ZnO nanoparticles and their catalytic activity for the removal of hazardous organic dyes. *J. Mol. Liq.* **2024**, *395*, 123783.
19. Awasthi, N.; Singh, A.K.; Jain, R.K.; et al. Degradation and detoxification of endosulfan isomers by a defined co-culture of two Bacillus strains. *Appl. Microbiol. Biotechnol.* **2003**, *62*, 279–283. https://doi.org/10.1007/s00253-003-1241-7.
20. Debnath, B.; Haldar, D.; Purkait, M.K. Environmental Remediation by Tea Waste and Its Derivative Products: A Review on Present Status and Technological Advancements. *Chemosphere* **2022**, *300*, 134480. https://doi.org/10.1016/j.chemosphere.2022.134480.
21. Jia, J.; Cai, M.; Li, X.; et al. Performance and mechanism of chitosan-modified La-based MOF nanocomposites for high-efficiency adsorption of azo anion dye Congo red. *J. Ind. Eng. Chem.* **2025**, *143*, 740–751
22. Nasar, A. Utilization of Tea Wastes for the Removal of Toxic Dyes from Polluted Water: A Review. *Biomass Convers. Biorefinery* **2023**, *13*, 1399–1415. https://doi.org/10.1007/s13399-020-01205-y.
23. Shah, S.K.; Pate, V.A. Tea Production in India: Challenges and Opportunities. *J. Tea Sci. Res.* **2016**, *6*, 1–6. https://doi.org/10.5376/jtsr.2016.06.0005.
24. Guo, S.; Kumar Awasthi, M.; Wang, Y.; et al. Current Understanding in Conversion and Application of Tea Waste Biomass: A Review. *Bioresour. Technol.* **2021**, *338*, 125530. https://doi.org/10.1016/j.biortech.2021.125530.
25. Hussain, S.; Salman, M.; Al-Ahmary, K.M.; et al. Synthesis of Potential Adsorbent for Removal of Malachite Green Dye Using Alginate Hydrogel Nanocomposites. *Int. J. Biol. Macromol.* **2025**, *289*, 138816. https://doi.org/10.1016/j.ijbiomac.2024.138816.
26. Pal, I.; Chopra, L.; Rajendran, S.; et al. Novel synthesis of GG-g-PAN based hydrolyzed products exclusion of Congo red and methylene blue dyes undertaken aqueous medium for spectroscopic investigations. *J. Mol. Liq.* **2024**, *416*, 126346.
27. Farasati Far, B.; Naimi-Jamal, M.R.; Jahanbakhshi, M.; et al. Decontamination of Congo red dye from aqueous solution using nanoclay/chitosan-graft-gelatin nanocomposite hydrogel. *J. Mol. Liq.* **2024**, *395*, 123839. https://doi.org/10.1016/j.molliq.2023.123839.
28. Hussain, S.; Anjali, K.P.; Hassan, S.T.; et al. Waste Tea as a Novel Adsorbent: A Review. *Appl. Water Sci.* **2018**, *8*, 165. https://doi.org/10.1007/s13201-018-0824-5.
29. Rasilingwani, T.E.; Gumbo, J.R.; Masindi, V.; et al. Removal of Congo red dye from industrial effluents using metal oxide-clay nanocomposites: Insight into adsorption and precipitation mechanisms. *Water Resour. Ind.* **2024**, *31*, 100253.
30. Kushwaha, A.K.; Gupta, N.; Chattopadhyaya, M.C. Removal of cationic methylene blue and malachite green dyes from aqueous solution by waste materials of Daucus carota. *J. Saudi Chem. Soc.* **2014**, *18*, 200–207. https://doi.org/10.1016/j.jscs.2011.06.011.
31. Mittal, A.; Mittal, J.; Malviya, A.; et al. Adsorption of Hazardous Dye Crystal Violet from Wastewater by Waste Materials. *J. Colloid Interface Sci.* **2010**, *343*, 463–473. https://doi.org/10.1016/j.jcis.2009.11.060.
32. Osmari, T.A.; Gallon, R.; Schwaab, M.; et al. Statistical Analysis of Linear and Non-Linear Regression for the Estimation of Adsorption Isotherm Parameters. *Adsorpt. Sci. Technol.* **2013**, *31*, 433–458. https://doi.org/10.1260/0263-6174.31.5.433.
33. Soni, S.; Bajpai, P.K.; Mittal, J.; et al. Utilisation of Cobalt Doped Iron Based MOF for Enhanced Removal and Recovery of Methylene Blue Dye from Waste Water. *J. Mol. Liq.* **2020**, *314*, 113642. https://doi.org/10.1016/j.molliq.2020.113642.
34. Soni, S.; Bajpai, P.K.; Bharti, D.; et al. Removal of Crystal Violet from Aqueous Solution Using Iron Based Metal Organic Framework. *Desalination Water Treat.* **2020**, *205*, 386–399. https://doi.org/10.5004/dwt.2020.26387.
35. Rai, N.; Sinha, D.K.; Soni, S.; et al. Biosorption study of basic dye using aerial part of widely growing weed Chenopodium album. *Desalination Water Treat.* **2023**, *314*, 276–285. https://doi.org/10.5004/dwt.2023.30112.
36. Delpiano, G.R.; Tocco, D.; Medda, L.; et al. Adsorption of Malachite Green and Alizarin Red S Dyes Using Fe-BTC Metal Organic Framework as Adsorbent. *Int. J. Mol. Sci.* **2021**, *22*, 788. https://doi.org/10.3390/ijms22020788.
37. Svidrytski, A.; Hlushkou, D.; Thommes, M.; et al. Modeling the Impact of Mesoporous Silica Microstructures on the Adsorption Hysteresis Loop. *J. Phys. Chem. C* **2020**, *124*, 21646–21655. https://doi.org/10.1021/acs.jpcc.0c07571.

38. Patel, A.; Soni, S.; Mittal, J.; et al. Sequestration of Crystal Violet from Aqueous Solution Using Ash of Black Turmeric Rhizome. *Desalination Water Treat.* **2021**, *220*, 342–352. https://doi.org/10.5004/dwt.2021.26911.
39. Tahir, S.S.; Rauf, N. Removal of Cationic Dye from Aqueous Solutions by Adsorption onto Bentonite Clay. *Chemosphere* **2006**, *63*, 1842–1848. https://doi.org/10.1016/j.chemosphere.2005.10.033.
40. Hameed, B.H.; Ahmad, A.A. Batch Adsorption of Methylene Blue from Aqueous Solution by Garlic Peel, an Agricultural Waste Biomass. *J. Hazard. Mater.* **2009**, *164*, 870–875. https://doi.org/10.1016/j.jhazmat.2008.08.084.
41. Mansour, M.S.; Ossman, M.E.; Farag, H.A. Removal of Cadmium(II) Ion from Wastewater by Adsorption onto Polyaniline Coated on Sawdust. *Desalination* **2011**, *272*, 301–305. https://doi.org/10.1016/j.desal.2011.01.037.
42. Duff, D.G.; Ross, S.M.C.; Vaughan, D.H. Adsorption from Solution: An Experiment to Illustrate the Langmuir Adsorption Isotherm. *J. Chem. Educ.* **1988**, *65*, 815. https://doi.org/10.1021/ed065p815.
43. Rai, N.; Verma, A.; Kumar, S.; et al. Affordable Sequestration of Basic Fuchsin Using Ferrocene Impregnated Iron-Based Metal-Organic Frameworks. *Part. Sci. Technol.* **2026**, *44*, 95–110. https://doi.org/10.1080/02726351.2025.2567434.
44. Rai, N.; Soni, S.; Verma, A.; et al. Sequestration of a Cationic Dye Using Graphene Oxide as Adsorbent. *Desalination Water Treat.* **2023**, *307*, 180–189. https://doi.org/10.5004/dwt.2023.29846.
45. Senthil Kumar, P.; Palaniyappan, M.; Priyadharshini, M.; et al. Adsorption of Basic Dye onto Raw and Surface-Modified Agricultural Waste. *Environ. Prog. Sustain. Energy* **2014**, *33*, 87–98. https://doi.org/10.1002/ep.11756.
46. Zhao, X.; Liu, S.; Tang, Z.; et al. Synthesis of Magnetic Metal-Organic Framework (MOF) for Efficient Removal of Organic Dyes from Water. *Sci. Rep.* **2015**, *5*, 11849. https://doi.org/10.1038/srep11849.
47. Khan, F.A.; Dar, B.A.; Farooqui, M. Characterization and adsorption of malachite green dye from aqueous solution onto *Salix alba* L. (Willow tree) leaves powder and its respective biochar. *Int. J. Phytoremediation* **2023**, *25*, 646–657. https://doi.org/10.1080/15226514.2022.2098909.
48. Jabar, J.M.; Odusote, Y.A. Utilization of prepared activated biochar from water lily (Nymphaea lotus) stem for adsorption of malachite green dye from aqueous solution. *Biomass Convers. Biorefinery***2024**, *14*, 5999–6010. https://doi.org/10.1007/s13399-021-01399-9.
49. Hammud, H.H.; Hammoud, M.H.; Hussein, A.A.; et al. Removal of Malachite Green Using Hydrochar from PALM Leaves. *Sustainability* **2023**, *15*, 8939. https://doi.org/10.3390/su15118939.
50. Arora, C.; Verma, A.; Soni, S.; et al. Recent Advances in Sequestration of Dyes Using Metal-Organic Frameworks. *Chem. Pap.* **2025**, *79*, 3513–3545. https://doi.org/10.1007/s11696-025-04025-4.
51. Özkan, U.; Bayram, O.; Şahin, H.T. Effect of Sorption Parameters on the Removal of Malachite Green with Modified Juniperus excelsa Cone Biochar. *Biomass Convers. Biorefinery* **2025**, *15*, 25093–25106. https://doi.org/10.1007/s13399-025-06797-x.
52. Yıldırım, G.M.; Bayrak, B. The synthesis of biochar-supported nano zero-valent iron composite and its adsorption performance in removal of malachite green. *Biomass Convers. Biorefinery* **2022**, *12*, 4785–4797. https://doi.org/10.1007/s13399-021-01501-1.
53. Belcaid, A.; Beakou, B.H.; Bouhsina, S.; et al. Biosorption of Cobalt and Chromium from Wastewater Using Manganese Dioxide and Iron Oxide Nanoparticles Loaded on Cellulose-Based Biochar: Modeling and Optimization with Machine Learning (Artificial Neural Network). *Int. J. Biol. Macromol.* **2024**, *282*, 136855. https://doi.org/10.1016/j.ijbiomac.2024.136855.
54. Jabar, J.M.; Adebayo, M.A.; Odusote, Y.A.; et al. Valorization of microwave-assisted H_3PO_4-activated plantain (*Musa paradisiacal* L.) leaf biochar for malachite green sequestration: models and mechanism of adsorption. *Results Eng.* **2023**, *18*, 101129. https://doi.org/10.1016/j.rineng.2023.101129.
55. Kameliya, J.; Verma, A.; Dutta, P.; et al. Layered Double Hydroxide Materials: A Review on Their Preparation, Characterization, and Applications. *Inorganics* **2023**, *11*, 121. https://doi.org/10.3390/inorganics11030121.